

Electrical impedance of ethylene-carbon monoxide/propylene-carbon monoxide (*EPEC-69*) thermoplastic polyketone

Saadi Abdul Jawad · Adnan S. Abu-Surrah ·
Mufeed Maghrabi · Ziad Khattari ·
Manar Al-Obeid

Received: 26 September 2010/Accepted: 30 November 2010/Published online: 18 December 2010
© Springer Science+Business Media, LLC 2010

Abstract Electrical impedance technique was employed to investigate the electrical properties of ethylene-carbon monoxide/propylene-carbon monoxide terpolymer (*EPEC-69*). The measurements were performed in the frequency range 0.1–10⁵ Hz and in the temperature range 30–110 °C. The results reveal that the dielectric constant, loss factor, modulus, and ac conductivity are dependent of frequency and temperature. A Debye relaxation peak was detected in the plot of Z'' versus frequency where the activation energy was determined and found to be 1.26 eV. When the surface phenomenon effects were separated using the imaginary part of the complex admittance a second dielectric dispersion was observed in the low frequency region. Two models were proposed from the impedance measurements depending on temperature range.

Introduction

Alternating polyketones represent a new family of organic polymers that offers a combination of useful chemical and physical characteristics such as photodegradability, biodegradability, chemical resistance, and ease of functionalization [1, 2]. Such properties can also be modified by changing the nature of the monomer [3, 4]. Developments in palladium(II) catalyzed copolymerization of olefins with carbon monoxide led to co- and terpolymers with highly

defined molecular weight, and stereo- and regioregularity [5–8].

The choice of appropriate reaction conditions and the design of metal catalyst allow to tailor the copolymer structure and, as a result, the bulk properties of the material: from highly crystalline thermoplastics to high molecular weight elastomers [9]. Some correlation of copolymer composition with morphology and deformation behavior has been obtained using co- and terpolymers of carbon monoxide with higher 1-olefins [10–12]. When the molar ratio of ethylene-CO (E-CO) to propylene-CO (P-CO) in the terpolymer is less than 50%, the material exhibits excellent elastic properties, while above this ratio the terpolymers are typical crystalline thermoplastics. Polyketone terpolymers which are dominated by a high molar ratio of E-CO to P-CO units (5–10% P-CO) have been commercialized under the trade names Carlion for Shell and Ketonex for British PetrolEum.

This research investigates the dielectric behavior of the alternating ethylene-carbon monoxide (E-CO)/propylene-carbon monoxide (P-CO) polyketone terpolymer with 69% E-CO units (*EPEC-69*) using impedance spectroscopy. This technique has been used extensively in recent years to investigate and characterize the electrical properties of solid polymers where different electrical parameters can be determined [13–24]. The material can be characterized by the equivalent circuit model composed of resistors and capacitors and other elements. The bulk dc conductivity can be determined from the complex plot of the real and imaginary parts of the complex impedance. In addition, the real part of ac conductivity can be determined from the dielectric loss data. The measurements were carried out in the frequency range 0.1–10⁵ Hz and in the temperature range 30 up to 110 °C. A comparative analysis of the complex dielectric constant, impedance, admittance,

S. A. Jawad (✉) · M. Maghrabi · Z. Khattari · M. Al-Obeid
Department of Physics, Hashemite University,
PO Box 150459, Zarqa 13115, Jordan
e-mail: saadi@hu.edu.jo

A. S. Abu-Surrah
Department of Chemistry, Hashemite University,
P.O. Box 150459, Zarqa 13115, Jordan

modulus, and the real part of ac conductivity was presented and discussed.

Experimental

Materials

Ethylene-carbon monoxide (E-CO)/propylene-carbon monoxide (P-CO) terpolymer (*EPEC-69*) with 69% E-CO units was prepared following a previously published procedure [11, 12]. The structure of alternating polyketone terpolymer is shown in Fig. 1. Analysis by infrared spectroscopy (IR), gel permeation chromatography (GPC), and differential scanning spectroscopy (DSC) is as follows: (IR(cm^{-1}): ν CO = 1706; Mw = 12.0×10^5 (Mw/Mn = 2.9); DSC: T_g = 14.1 °C, T_m = 53 °C, ΔH = 3.7 J/g). (Thermal gravimetric analysis (TGA): $T(50\%) \approx 400$ °C. Uniform films of the terpolymer were cast from a CH_2Cl_2 solution.

Impedance measurements

Ac impedance measurements were carried out in the frequency range 1– 10^5 Hz in the temperature range 30 (above T_g and less than T_m) to 110 °C using a Solarton-1260 Impedance/Gain Phase Analyzer with a 1,296 dielectric interface. Two software packages, Z-60 and Z-View were used to maximize the performance and data handling of the system. By measuring the amplitude and the phase shift of the resulting current, one can calculate the real (Z') and imaginary (Z'') components of the complex impedance. From the calculated values of Z' and Z'' the real and imaginary components of dielectric constant, electric modulus, and admittance were determined and plotted as a function of frequency at different temperatures.

Results and discussion

Figure 2 represents the variation of the real part of the impedance Z' with frequency at different temperatures. The figure shows a significant decrease in Z' values with increasing frequency for all temperatures investigated in

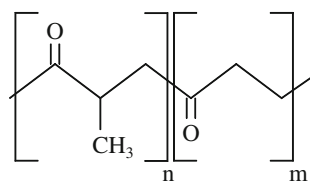


Fig. 1 The structure of ethylene-carbon monoxide (E-CO)/propylene-carbon monoxide (P-CO) terpolymer with 69% E-CO units (*EPEC-69*)

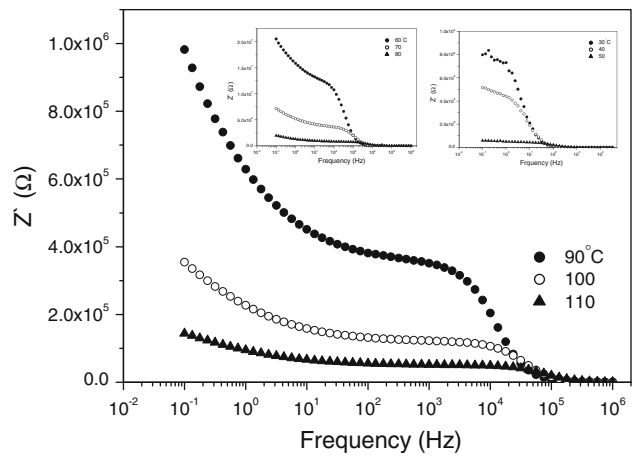


Fig. 2 Variation of the real component of complex impedance (Z') with frequency at different temperatures

this study. It should be noted that, the frequency and temperature dependence of Z' shows two transitions or switch in behavior from capacitive-like to a resistive-like behavior. The first transition was observed in the frequency range (0.1–10 Hz) for temperatures above 60 °C, where Z' increases significantly with a decrease in frequency. In the frequency range 10– 10^3 Hz, Z' is nearly independent of frequency. This observation suggests that a leakage current may exist in the bulk material which makes the sample more ohmic. The second transition occurs in the frequency range 10^3 Hz to less than 10^5 Hz, where the material shows more capacitive behavior. Moreover, Z' decreases dramatically in this range with increasing frequency, and varies almost with the inverse of frequency. At frequencies above 10^5 Hz, all Z' values merge for all temperatures, which clearly indicates the presence of space charge polarization effect at low frequencies in the materials, and this effect is diminished at higher frequencies [25, 26].

The significant increase in Z' with decreasing frequency is associated with relaxation processes as shown in Fig. 3, which represents the variation of Z'' with frequency at different temperatures. It shows a broad relaxation peak with a considerable decrease in its magnitude and a clear shift in the relaxation peak maximum toward the higher frequency with increasing temperature. An indication of another relaxation peak in the low frequency region was observed at temperatures higher than 60 °C, which is associated with a significant increase in Z' with a decrease in frequency.

To study this phenomenon closely, a complex impedance plot of Z'' versus Z' is plotted as shown in Fig. 4, the plot yields a single semi circle centered at $R_s + R_p/2$, 0 with radius $R_p/\sqrt{2}$ according to the relation $(Z'' - (R_s + R_p/2))^2 + Z'^2 = R_p^2/2$, where the subscripts p and s refer to the equivalent parallel and series circuits, respectively. The angular frequency ω_{\max} of the peak maxima and the centers

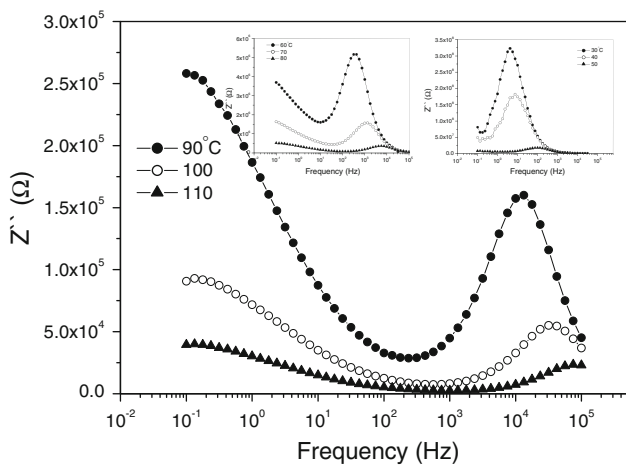


Fig. 3 Variation of the imaginary component of complex impedance (Z'') with frequency at different temperatures

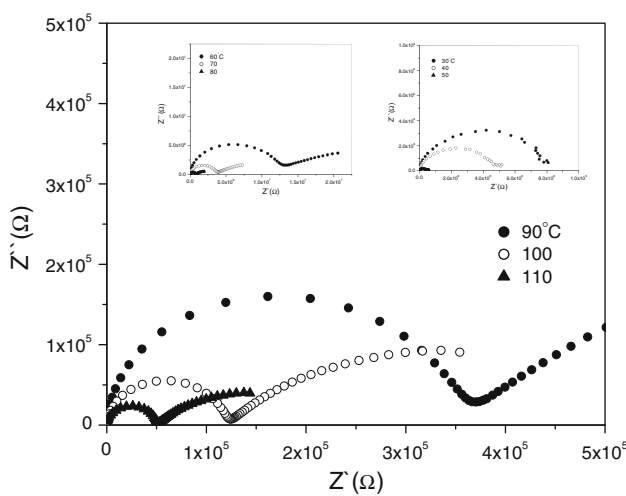


Fig. 4 Complex impedance plot at different temperatures

of the semi circles coincide, and are given by the reciprocal of the conductivity relaxation time (τ) according to the relation $\omega_{\max} = 2\pi f_{\max} = 1/\tau = \sigma \epsilon_0 \epsilon''$, where σ corresponds to the dc conductivity, ϵ_0 is the permittivity of free space and ϵ'' is the dielectric loss. The diameter of the semi circle corresponding to the bulk resistance of the sample decreases with increasing temperature indicating an activated conduction mechanism. At temperature above 60 °C an arc (a portion of semicircle) was observed in the low frequency region.

The high frequency semicircle is related to the conduction mechanism and the low frequency arc is attributed to the grain boundaries in the system. Measuring the diameter of the semicircles allow us to determined dc conductivity of the material from the relation $\sigma = 1/R_p (A/d)$, where A is the area of the sample and d is the thickness.

The calculated values are plotted as shown in Fig. 5. The dc conductivity increased slightly with increasing

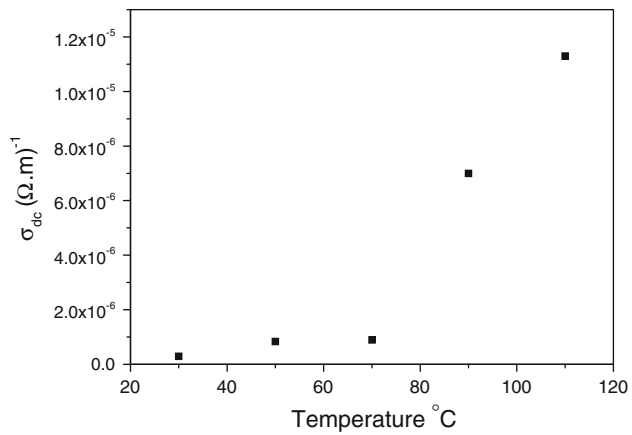


Fig. 5 Variation of dc conductivity with temperature calculated from Z'' versus Z'

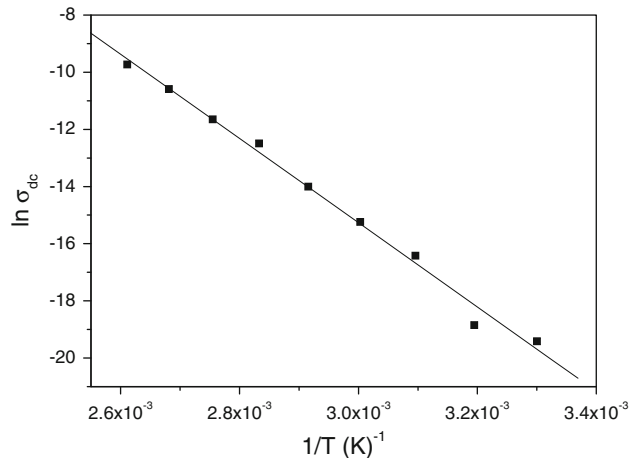


Fig. 6 Variation of dc conductivity with $1/T$ calculated from Z'' versus Z'

temperature up to about 70 °C and then a significant increase was observed with increasing temperature to attain a value of $6 \times 10^{-5} (\Omega \cdot m)^{-1}$ at 60 °C. The dc-conductivity dependence on temperature was found to follow an Arrhenius equation in the form $\sigma = \sigma_0 \exp(-\Delta E/kT)$ where ΔE is the activation energy, k is the Boltzmann constant and T is the absolute temperature. Figure 6 shows the logarithmic plot of the dc conductivity as a function of the reciprocal temperature. The nature of conductivity variation with rise in temperature together with a typical Arrhenius-type behavior suggests that the electrical conduction in the material is thermally activated. The activation energy, calculated from the slope of the graph was found to be 1.26 ± 0.02 eV.

The equivalent circuits used to fit the experimental data are shown in Fig. 7. The figure shows representative examples of the fit for temperatures 30 (Fig. 7a) and 100 °C (Fig. 7b). For temperature above 70 °C the

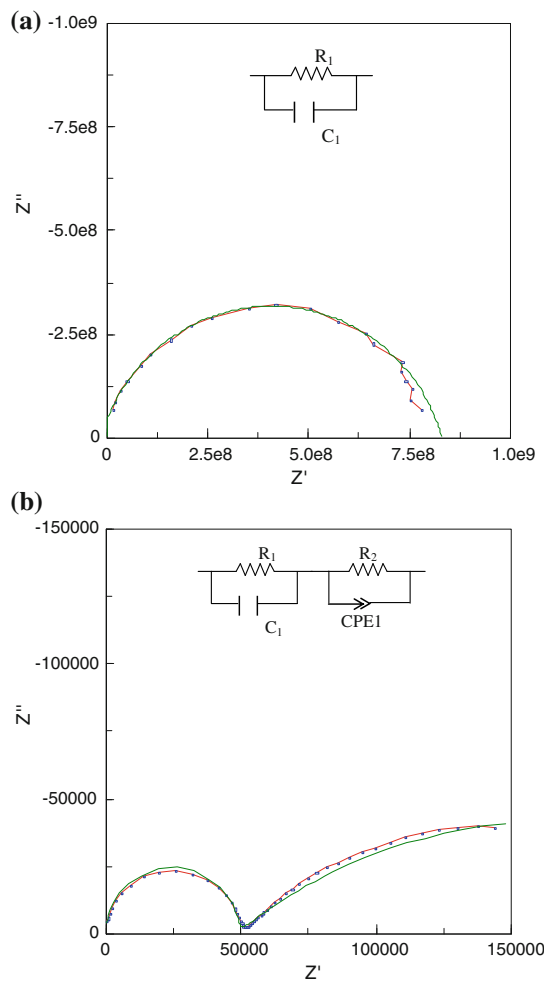


Fig. 7 Proposed equivalent model **a** at temperature 30°C and **b** at 100°C

equivalent circuit consists from two networks. The first circuit is RC in parallel which represents the high frequency data. The second circuit consists of R, and CPE (constant phase element) is connected with the first one. The CPE is used in a model in place of a double layer capacitor to compensate for non-homogeneity in the system [27]. Excellent fit with the proposed model was obtained with the experimental data with an average error less than 2%.

The appearance of a small arc in the complex plot of impedance gives an indication of another relaxation process in this material. In order to observe this relaxation, the bulk and the surface phenomenon effects on the dielectric dispersion should be separated, and this can be achieved using the imaginary part of the complex admittance [28, 29]. The real and imaginary parts of the complex impedance are related through the relation:

$$Y^* = \frac{1}{Z^*} = Y' - iY'' = \frac{Z'}{Z'^2 + Z''^2} - i \frac{Z''}{Z'^2 + Z''^2}$$

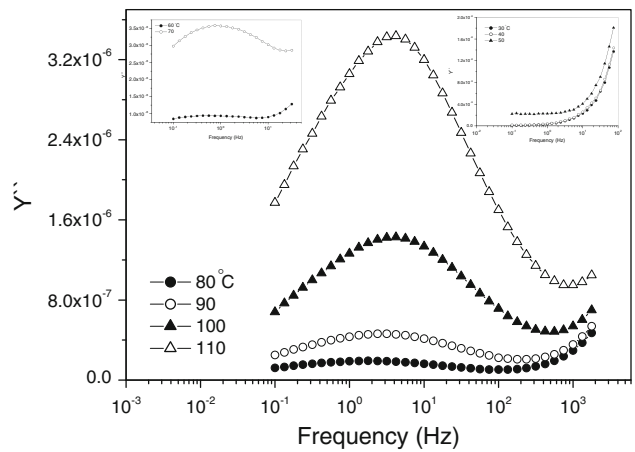


Fig. 8 Variation of the imaginary component of complex admittance (Y'') with frequency at different temperatures

In this equation Z' appears in Y'' equation in the denominator to the second power, its density to overwhelm the loss factor is minimized, therefore, a plot of Y'' as a function of frequency in the frequency range 0.01–100 Hz is shown in Fig. 8. Any relaxation peak in this range of frequency can be detected in the plot of Y'' versus frequency. Figure 8 shows a well-defined relaxation peak at temperature higher than 60°C with a slight shift to higher frequency with increasing temperature. The intensity of the relaxation peak increases dramatically with increasing temperature. Godovskiy et al. [30] found two melting peaks in the DSC spectrum of this material. The first at 55°C and they assigned this melting peak to the blockiness of the terpolymer. This may explain the presence of such a peak in the plot of Y'' versus frequency. Therefore, this peak can be associated with the partially melting of the crystalline phases, which release the constraints in the molecules at this temperature and facilitate the molecular mobility above this temperature. On other hand, the ac conductivity is both frequency- and temperature- dependent and increases in the measured temperature and frequency range as shown in Fig. 9. The influence of temperature is more pronounced in the low frequency region. In general, the ac conductivity can be presented by an empirical relation in the form $\sigma_{ac}(\omega) = A \omega^s$, where A is a complex constant, and s is the exponent of the angular frequency [20]. The graph of ac conductivity shows two distinct regions in the measured frequency. The values of the exponent s can be determined for each region from the slope of the plot of $\log \sigma_{ac}$ versus $\log \omega$. The calculated values of s increases with temperature and it is less than unity for both regions. However, the change in the slope takes place at a particular frequency which shifts to a higher frequency with an increase in temperature.

In order to investigate the dielectric processes in more details, the dielectric permittivity and the electric modulus

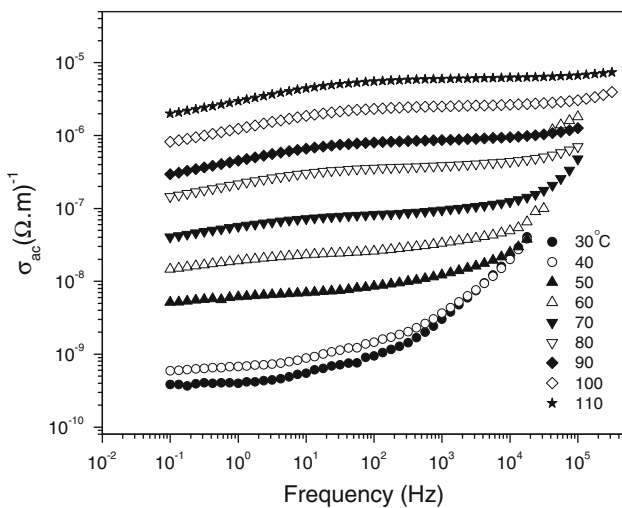


Fig. 9 Variation of ac conductivity with frequency at different temperatures

were determined from the measured values of the impedance using the following relations [15]:

$$M^* = (\varepsilon^*)^{-1} = M' - iM''$$

where $\varepsilon^* = \varepsilon' - i\varepsilon''$

$$\varepsilon' = \frac{-Z''}{(Z'^2 + Z''^2)\omega C_0}$$

and

$$\varepsilon'' = \frac{-Z''}{(Z'^2 + Z''^2)\omega C_0}$$

then,

$$M' = \frac{\varepsilon'}{(\varepsilon'^2 + \varepsilon''^2)}$$

$$M'' = \frac{\varepsilon''}{(\varepsilon'^2 + \varepsilon''^2)}$$

Fig. 10 shows the frequency-dependent of the real part of the complex dielectric constant at different temperature in the frequency range 0.1– 10^5 Hz. At low frequency, the values of the real part (ε') are sharply increases with decreasing frequency. However, a similar behavior of dielectric loss (ε'') was observed as shown in Fig. 11.

The high values of ε' and ε'' at low frequency may be interpreted as the accumulation of charges at the interface between the sample and the electrodes which gives a space charge polarization [31, 32]. With increasing frequency, the dipoles in the sample cannot reorient themselves fast enough to respond to the applied electric field resulting in the decrease of both ε' and ε'' . Therefore, no relaxation peak was observed in the plot of ε'' with frequency as shown in Fig. 11. In order to observe the relaxation peak

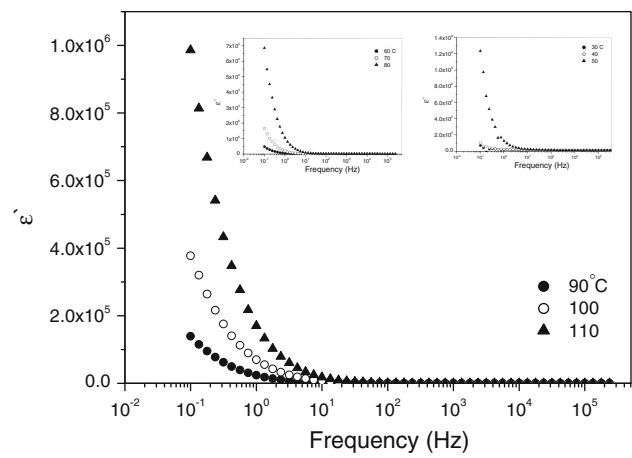


Fig. 10 Variation of dielectric loss (ε'') with frequency at different temperatures

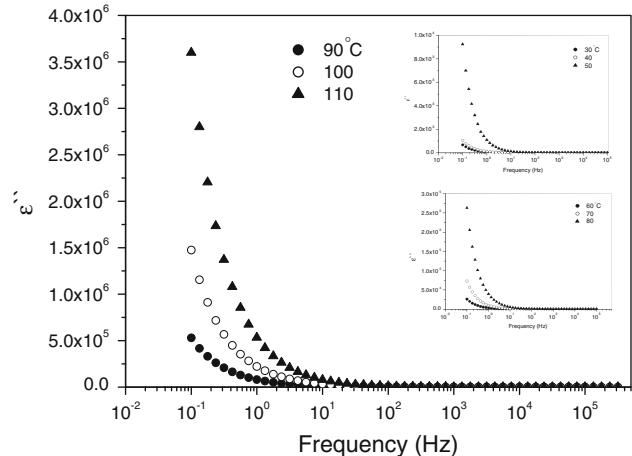


Fig. 11 Variation of loss factor (ε'') with frequency at different temperatures

the effect of electrode polarization and conductivity relaxation time must be extracted. This can be achieved by following the electric modulus approach, since the electric modulus corresponds to the relaxation on the electric field in the material when the electric displacement remains constant. This approach can be effectively used to separate out electrode effects which mask the dielectric relaxation.

Figure 12 shows the plot of M' with frequency at different temperatures. At temperatures above 60 °C, the value of M' approaches zero in the low frequency region and increases with increasing frequency to attain nearly a constant value corresponding to M_∞ for all temperatures. This is however, supports the conduction phenomena due to short range mobility [33]. This conclusion may further explain the dramatic increase in ε'' at low frequency which overlap any relaxation process.

Figure 13 shows M'' as a function of frequency at different temperatures. A well-defined broad relaxation peak

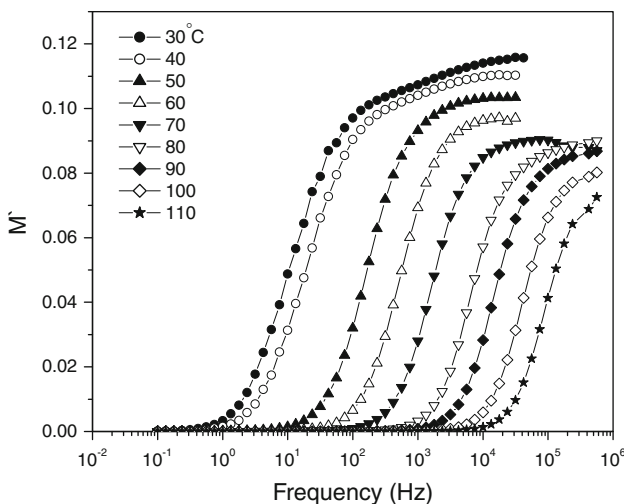


Fig. 12 Variation of the real component of complex modulus (M') with frequency at different temperatures

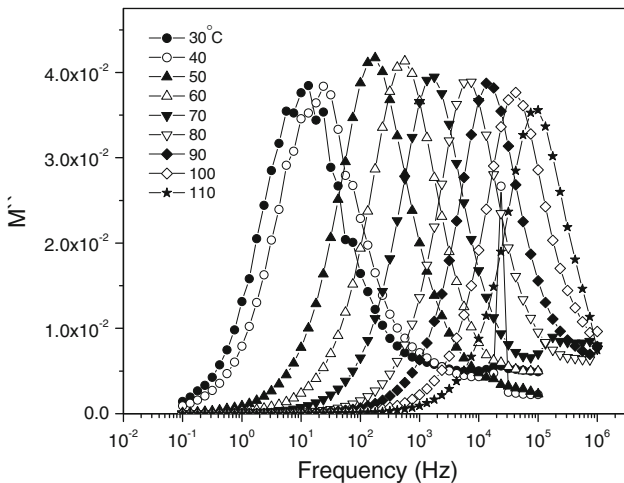


Fig. 13 Variation of the imaginary component of complex modulus (M'') with frequency at different temperatures

together with a systematic shift in frequency maximum to higher frequency with increasing temperature were observed, indicating that the active conduction is associated with dipole orientation.

Conclusions

The dielectric behavior of ethylene-carbon monoxide (E-CO)/propylene-carbon monoxide (P-CO) terpolymer with 69% E-CO units (*EPEC-69*) reveals two distinct regions. The first region is characterized by the slightly change in the ac- and dc- conductivity with temperature and frequency at temperatures less than its T_m . Above this temperature (the second region), a dramatic change in all the

dielectric variables with frequency and temperature was observed. The electric modulus approach reveals the relaxation process which was masked in the intermediate frequency in the plot of the dielectric loss. Moreover, the low frequency relaxation was only observed if the imaginary part of admittance is plotted as a function of frequency.

Acknowledgement Financial support by the Hashemite University is gratefully acknowledged. The authors would like to thank Mr. Abedal-Monim M. Said for carrying out the DSC measurements.

References

- Foullerat DP, Hild S, Mücke A, Rieger B (2004) *Macromol Chem Phys* 205:374
- Sen A, Jiang Z, Chen JT (1989) *Macromolecules* 22:2012
- Sunjuk M, Al-Noaimi M, Al-Degs YS, Al-Qirem T, Lindner E, Abu-Surrah AS (2009) *J Polym Sci* 47:6711
- Auer M, Kettunen M, Abu-Surrah AS, Wilen SCE, Leskelä M (2004) *Polym Inter* 53:2015
- Abu-Surrah AS, Rieger B (1996) *Angew Chem Int Ed Ing* 35:2475
- Anselment T M, Vagin S I, Rieger B (2008) *Dalton Trans* 4537
- Consiglio G (2003) In: "Late Transition Metal Polymerization Catalysis" Rieger B, Baugh L S, Kacker S, Striegler S (eds.) Wiley-VCH, Weinheim
- Drent E, Budzelaar HM (1999) *Chem Rev* 96:663
- Abu-Surrah AS, Rieger B (1999) *Topics in Cat* 7:165
- Abu-Surrah AS, Wursche R, Rieger B (1997) *Macromol Chem Phys* 198:1197
- Abu-Surrah AS, Eckert G, Pechhold W, Wilke W, Rieger B (1996) *Macromol Rapid Commun* 17:559
- Rieger B, Abu-Surrah A S, Wursche R Ger. R (1996) Offen. DE 196 49: 072, WO 98/23665: 42217
- Mount A R, Robertson M T (1999) Chapter 11 AC impedance spectroscopy of polymer films-An overview. *Comprehensive Chemical Kinetics*, volume 37 p 439
- Jiang J, H.Ai. L (2010). *Physica B* 405: 263
- Pittini YY, Daneshvari D, Pittini R, Vaucher S, Roh L, Leparoux S, Leuenberger H (2008) *Eur Polym J* 44:1191
- Noto Vito Di, Vittadello, Michele (2002) Solid state ionics. 147, Issues 3–4: 309
- Raja V, Sharma AK, Narasimha Rao VVR (2004) *Mater Lett* 58(26):3242
- Al-Ramadin Y, Ahmad M, Zihlif Z, Alnajjar A, Abdul Jawad S, Musto P, Ragosta G, Martuscelli E (1999) *Polymer* 40:3877
- Abdul Jawad S, Ahmad MS (1993) *Mater Lett* 17:91
- El-Ghanem H, Attat H, Sayed H, Abdul Jawad S (2006) *Inter J Polym Mater* 55:663
- Buenfeld NR, Zhang J (2000) *J Mater Sci* 35:39. doi:[10.1023/A:1004724128509](https://doi.org/10.1023/A:1004724128509)
- Torrents TM, Mason TO, Peled A, Shan Sp, Carboezi EJ (2001) *J Mater Sci* 36:4003. doi:[10.1023/A:101798608910](https://doi.org/10.1023/A:101798608910)
- Guofoneg K, Lee ND, Tewari SN (2006) *J Mater Sci* 41:6855. doi:[10.1007/s10853-006-0945-3](https://doi.org/10.1007/s10853-006-0945-3)
- Kim C-J, KWANGSOO NO (1993) *Mat Sci* 28:5765
- Suchaniz J (1998) *Mat Sci Eng* B55:114
- Sen S, Chowdhary RNP, Tarafdar A, Pramanik PJ (2006) *Appl Phys* 99(124):114
- Kyritsis A, Pissis P, Grammatikakis J (1995) *J Polym Sci Part B Polym Phys Ed* 33:1737

28. Havriliak SJ (1997) Dielectric and mechanical relaxation in materials, In: analysis interpretation and application to polymers, Hanser Publisher, Cincinnati
29. Pissis P, Kyritsis A (1997) Solid State Ionics 97:105
30. Godovsky YK, Konyukhova EV, Chvalun SN, Neverov VM, Abu-surrah AS, Rieger B (1999) Macromol Chem Phys 200:2636
31. Ravikiran YM, Lagare M, Sairam, Mallikarjuna N, Sreedhar B, Manohar S, Mazdiarmid A, Aminabhaui T (2006) Synth Met 156:1139
32. Hodge IM, Ngaik L, Moynihan CT (2005) J Non-Crystalline Solids 351:104
33. Mudarra M, Díaz-Calleja R, Belana J, Cañadas JC, Diego JA, Sellarès J, Sanchís MJ (2001) Polymer 2:1647